https://doi.org/10.1007/s11467-023-1367-2

RESEARCH ARTICLE

Spin transport of half-metal Mn_2X_3 with high Curie temperature: An ideal giant magnetoresistance device from electrical and thermal drives

Bin Liu[1, ‡], Xiaolin Zhang[1, 2, ‡], Jingxian Xiong[3], Xiuyang Pang[3], Sheng Liu[1], Zixin Yang[3], Qiang Yu[3, 5], Honggen Li[6], Sicong Zhu[1, 4,†], Jian Wu[3,‡]

[1] Hubei Province Key Laboratory of Systems Science in Metallurgical Process, The State Key Laboratory for Refractories and Metallurgy, Collaborative Innovation Center for Advanced Steels, International Research Institute for Steel Technology, Wuhan University of Science and Technology, Wuhan 430081, China

[2] Key Laboratory of Artificial Micro- and Nano-structures of Ministry of Education And School of Physical and Technology, Wuhan University, Wuhan 430072, China

[3] College of Advanced Interdisciplinary Studies, Nanhu Laser Laboratory, National University of Defense Technology, Changsha 410073, China

[4] Department of Mechanical Engineering, National University of Singapore, Singapore 117575, Singapore

[5] i-Lab & Key Laboratory of Nanodevices and Applications & Key Laboratory of Nanophotonic Materials and Devices, Suzhou Institute of Nano-Tech and NanoBionics, Chinese Academy of Sciences, Suzhou 215123, China

[6] Institute of Optical Science and Technology, School of Physics and Astronomy, Shanghai Jiao Tong University, Shanghai 200240, China

‡ These authors contributed equally to this work.

Corresponding author. E-mail: †sczhu@wust.edu.cn, ‡wujian15203@163.com

Supporting information

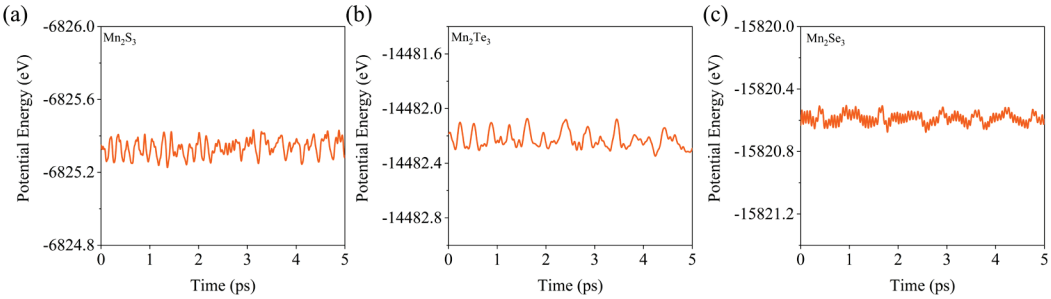

Fig. S1 Evolution of total energy of Mn_2X_3 monolayers from AIMD simulations at 300 K.

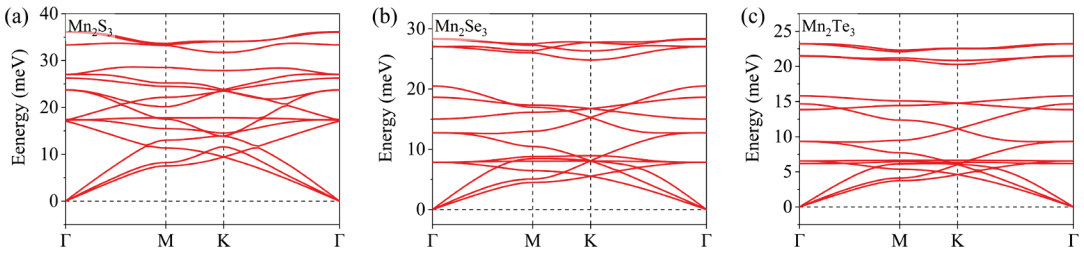

Fig. S2 Phonon dispersion of Mn_2X_3.

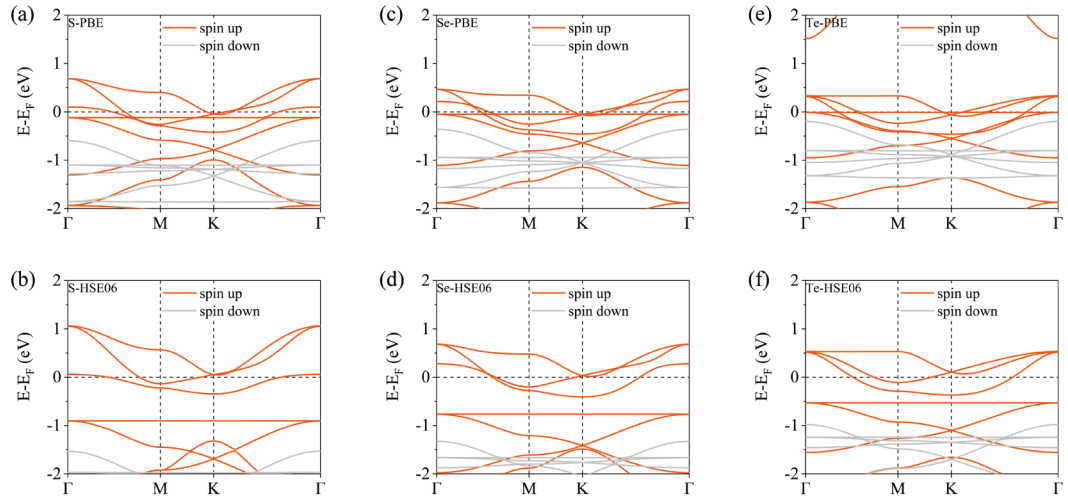

Fig. S3 Band structure of Mn_2X_3, Electronic band structure at the PBE level and at the HSE06 level for Mn_2X_3 monolayers. The horizontal line shows the Fermi level at zero eV.

Figure S3 presents the results of band structure calculations conducted using the PBE and HSE06 methods. The band structure analysis conducted using the HSE06 method reveals that monolayers of Mn_2S_3, Mn_2Se_3, and Mn_2Te_3 continue to exhibit half-metallic behavior. Despite the presence of a wider spin gap in the semiconductor channels as compared to the results obtained using the PBE method, these monolayers nevertheless demonstrate 100% spin polarization. This study serves as a solid foundation for further investigations on spin transport.

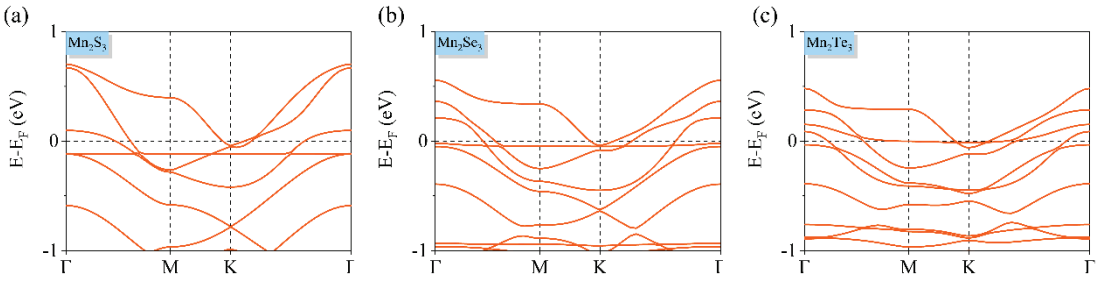

Fig. S4 Band structure of Mn_2X_3 with SOC.

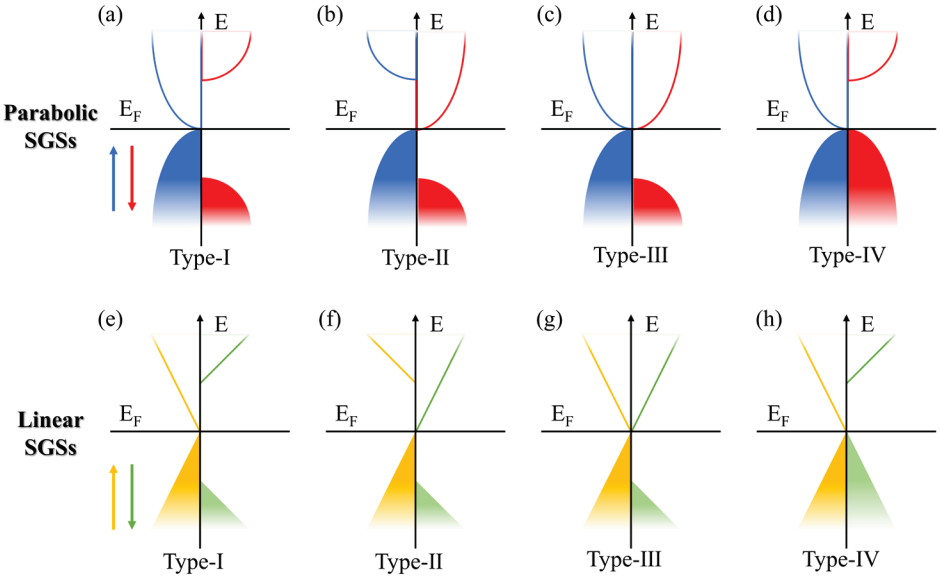

Fig. S5 Band structure diagram. Band structure diagram for **(a)** type-I PSGSs, **(b)** type-II PSGSs, **(c)** type-III PSGSs, **(d)** type-IV PSGSs, **(e)** type-I LSGSs, **(f)** type-II LSGSs, **(g)** type-III LSGSs, and (h) type-IV LSGSs, respectively.

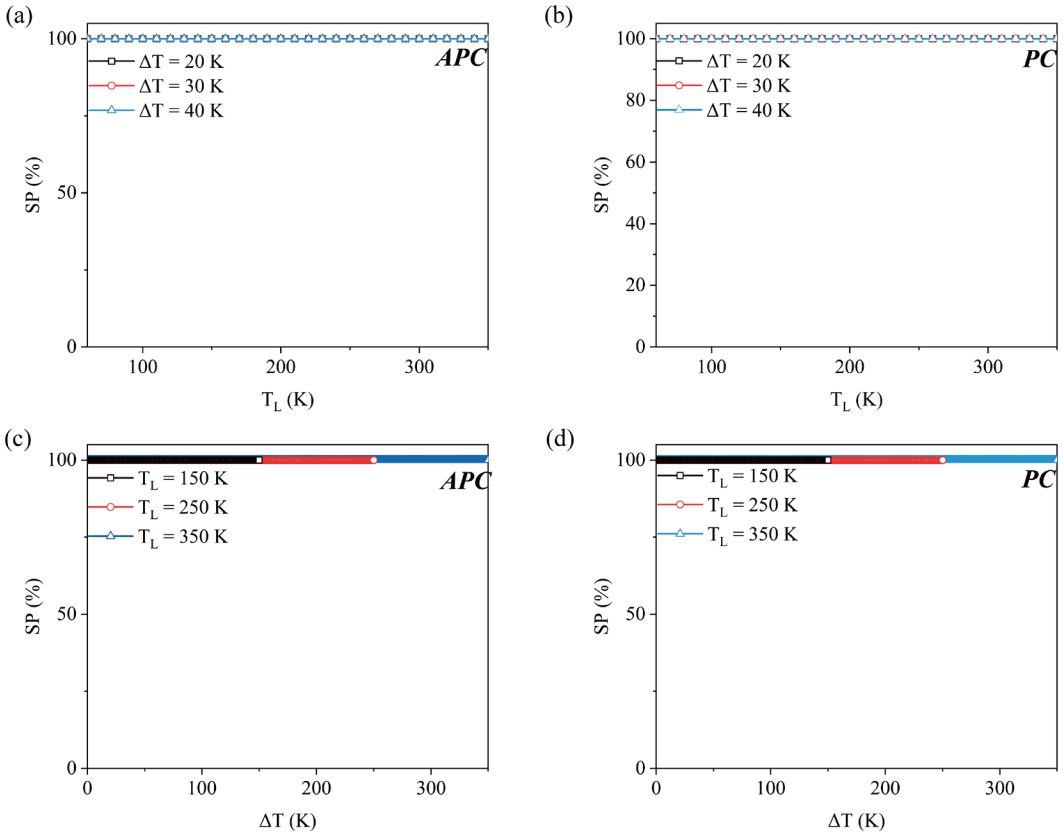

Fig. S6 Spin filtering effect under thermal transport.

Table S1 Calculated energy difference compared to ferromagnetic (FM) state (eV/f.u) in the FM state and three antiferromagnetic (AFM) states: Neel AFM (nAFM), stripe AFM (sAFM), and zigzag AFM (zAFM), and the lattice constant for Mn_2X_3 monolayers.

		FM (eV/f.u)	nAFM (eV/f.u)	sAFM (eV/f.u)	zAFM (eV/f.u)	*a* (Å)	*b* (Å)
GGA	Mn_2S_3	0	+0.50747	+0.3624	+0.190292	7.8	6.7
	Mn_2Se_3	0	+0.42646	+0.40024	+0.251805	7.4	6.4
	Mn_2Te_3	0	+0.303827	+0.316988	+0.212585	9.0	7.8
LDA	Mn_2S_3	0	+0.459347	+0.357745	+0.204125		
	Mn_2Se_3	0	+0.415977	+0.383208	+0.23752		
	Mn_2Te_3	0	+0.239	+0.27917	+0.203557		

The estimation of Curie temperature

The initial step in our analysis involves the application of the Heisenberg model to ascertain the magnetic exchange interactions among Mn magnetic ions. This is accomplished by employing a spin Hamiltonian:

$$H = -J_1 \sum_{i,j} S_i . S_j - J_2 \sum_{k,l} S_k . S_l - J_3 \sum_{p,q} S_p . S_q \quad (1)$$

where S_i is the spin vector each Mn atom, and J_1, J_2, and J_3 are the exchange-interaction parameters between the nearest neighbors, the second nearest neighbors and the third nearest neighbors, respectively. It should be noted that J_i (i=1, 2, 3) indicate the presence of ferromagnetic (FM) interactions, whereas negative values indicate the presence of antiferromagnetic (AFM) interactions. The energy of the spin orderings can be expressed by

$$E_{FM} = E_0 - (3J_1 + 6J_2 + 3J_3)S^2 \quad (2)$$

$$E_{Neel} = E_0 - (-3J_1 + 6J_2 - 3J_3)S^2 \quad (3)$$

$$E_{Stripy} = E_0 - (-1J_1 - 2J_2 + 3J_3)S^2 \quad (4)$$

$$E_{Zigzag} = E_0 - (1J_1 - 2J_2 - 3J_3)S^2 \quad (5)$$

where E_0 is the ground-state total energy independent of the spin configurations. For the Mn_2X_3 system, the evaluation of electron interaction is conducted through the assessment of Heisenberg exchange coupling between adjacent atoms. The exchange coefficient of Mn_2S_3 is notably higher compared to that of Mn_2Se_3 and Mn_2Te_3, and the outermost electrons of the S system in the same family are more active. Therefore, the exchange impact between electrons is observed to be more pronounced. Simultaneously, there is significant overlap between the broad p orbital of atom X and the d orbital of the Mn. The transition orbitals of Mn and S exhibit a comparatively facile behavior with respect to the movement of electrons. Additional research provides evidence that aligns with this perspective. This observation suggests a greater Curie temperature for the Mn_2S_3 crystal structure. As exemplified by the study conducted by Endo *et al.* [1], it was observed that in Mn systems, there is a propensity for Mn structures to display significant interactions with non-metallic elements. Additionally, the researchers made predictions regarding high Curie temperatures for materials based on Mn. Simultaneously, Wang et al. have also substantiated this perspective [2], and aligning with our finding. Further, the enhanced exchange coefficient suggests that the Mn_2S_3 system exhibits improved ability to sustain magnetic order as the ambient temperature rises [3]. Hence, it may be inferred that the Mn_2S_3 system has the potential to achieve a greater Curie temperature.

The estimation of the Curie temperature can be achieved through the utilization of Monte Carlo (MC) simulations after acquiring the magnetic exchange-interaction parameters J. It should be noted that the selection of the exchange-interaction parameter is limited to the nearest-neighboring interactions, as they exhibit significantly bigger magnitudes compared to those of the second and third nearest neighbors. In the MC simulations, a 50×50 supercell and 50000 MC steps for each temperature are employed and spins on all magnetic sites flip randomly.

References

1. T. Endo, Y. Doi, M. Wakeshima, K. Suzuki, Y. Matsuo, K. Tezuka, T. Ohtsuki, Y. J. Shan, and Y. Hinatsu, Magnetic properties of the melilite-type oxysulfide $Sr_2MnGe_2S_6O$: Magnetic interactions enhanced by anion substitution, *Inorganic Chemistry* 56, 2459 (2017)
2. C. Yu, X. Li, X. Li, and J. Yang, High Curie temperature and intrinsic ferromagnetic half-metallicity in Mn_2X_3 (X = S, Se, Te) nanosheets, *The Journal of Physical Chemistry Letters* 12, 11790 (2021)

3. Z. Wang, M. Zhang, Y. Ge, W. Wan, and Y. Liu, Monolayer MX_2 (M = Cr, Mn; X = Se, Te) with a square lattice: A ferromagnetic half-metal with high Curie temperature, *Results in Physics* 51, 106687 (2023)